138259-92-4; $[\mathrm{Rh_2(dpb)_4}]^+$, 99148-27-3; $[\mathrm{Rh_2(dpb)_4}]^{2+}$, 99165-18-1; $[\mathrm{Co_2(dpb)_4}]^{2+}$, 138259-93-5; Co, 7440-48-4; Rh, 7440-16-6.

Supplementary Material Available: For **1**–**3**, Tables SI–SIV, listing data collection and processing parameters, hydrogen atomic coordinates, complete bonding geometry, and anisotropic thermal parameters, and Figures S1–S8, showing packing diagrams, visible and near-IR spectra, and cyclic voltammograms (22 pages); tables of observed and calculated structure factors (35 pages). Ordering information is given on any current masthead page.

Contribution from the Laboratoire de Chimie Inorganique, URA No. 420, Université de Paris-Sud,
91405 Orsay, France, Laboratoire de Chimie des Métaux de Transition, URA No. 419,
75232 Paris, France, and Service National des Champ Intenses, UPR No. 5021, 38042 Grenoble, France

Weak Ferromagnetism in the Molecular Compound Cu(ta)(3-pic)$\cdot$H$_2$O (ta = Terephthalato, 3-pic = 3-Picoline). Crystal Structure of Cu(ta)(3-pic)$_2\cdot$0.5(3-pic)$\cdot$0.5CH$_3$OH

Evangelos Bakalbassis,[1a] Pierre Bergerat,[1a] Olivier Kahn,*[,1a] Suzanne Jeannin,[1b] Yves Jeannin,[1b] Yves Dromzee,[1b] and Maurice Guillot[1c]

Received May 29, 1991

The two compounds Cu(ta)(3-pic)$_2\cdot$0.5(3-pic)$\cdot$0.5CH$_3$OH (**1**) and Cu(ta)(3-pic)$\cdot$H$_2$O (**2**) have been synthesized, ta standing for terephthalato and 3-pic for 3-picoline. The crystal structure of **1** has been determined. **1** crystallizes in the monoclinic system, space group $P2_1/c$, with a = 9.703 (4) Å, b = 13.184 (8) Å, c = 19.825 (4) Å, β = 115.12 (2)°, and Z = 4. The structure consists of Cu(ta) infinite layers, to which the 3-pic molecules are perpendicular, and noncoordinated 3-pic and CH$_3$OH molecules. In the lattice the Cu(ta)(3-pic)$_2$ units are centrosymmetrically related, affording copper(II) pairs with a Cu$\cdots$Cu separation of 4.414 Å. Those pairs are linked together through terephthalate bridges. **1** spontaneously evolves in air to yield **2**. The copper(II) ions in **1** are magnetically isolated. In contrast, the magnetic properties of **2** are quite unusual. Magnetic susceptibility measurements together with EPR spectra and low-field (5 G) and high-field (up to 20 T) magnetization data lead to the following description: **2** consists of antiferromagnetically coupled copper(II) pairs with a singlet–triplet energy gap $J \approx -330$ cm^{-1}. In addition, antisymmetric interaction gives rise to a residual magnetic moment in the ground state. The pairs weakly couple through the terephthalate bridges in such a way that the pair magnetic moments align along the same direction. **2** exhibits a weak ferromagnetic transition at T_c = 2.8 K.

Introduction

More and more researchers working with open-shell molecules are interested by the bulk magnetic properties.[2] One of the main challenges in this field is then to design molecular-based compounds exhibiting a spontaneous magnetization. Spectacular results along this line have recently been reported.[3–14] Additionally, molecules with a high-spin multiplicity in the ground state have been described.[15–18]

To design molecular materials displaying a zero-field magnetization below a critical temperature T_c, one must assemble magnetic molecular units in such a way that the interaction between the local spin carriers at the scale of the lattice leads to a nonzero resulting spin. This result can be achieved under various conditions as follows: (i) All the interactions between nearest neighbors are ferromagnetic. If so, the local spins tend to align along the same direction and a ferromagnetic transition is expected to occur at a critical temperature T_c. (ii) All the interactions between nearest neighbors are antiferromagnetic, but owing to a noncompensation of the interacting local spins, the resulting spin is different from zero. If intra- and intermolecular interactions are not distinguished, this system is called a ferrimagnet and a magnetically ordered state with a spontaneous magnetization is again expected below the critical temperature T_c. (iii) All the spin carriers are similar and couple antiferromagnetically, with nevertheless a small canting, so that there is a nonzero resulting spin. If so, a weak ferromagnetic transition is expected at T_c. (iv) Finally, a nonzero resulting spin may arise from very complicated

---

(1) (a) Université de Paris-Sud. (b) URA No. 419. (c) UPR No. 5021.

(2) Gatteschi, D., Kahn, O., Miller, J., Palacio, F., Eds. *Molecular Magnetic Materials*; NATO ASI Series; Klüwer: Dordrecht, The Netherlands, 1991.

(3) Miller, J. S.; Calabrese, J. C.; Rommelmann, H.; Chittipeddi, S. R.; Zhang, J. H.; Reiff, W. M.; Epstein, A. J. *J. Am. Chem. Soc.* **1987**, *109*, 769.

(4) Miller, J. S.; Epstein, A. J.; Reiff, W. M. *Science* **1988**, *240*, 40; *Chem. Rev.* **1988**, *88*, 201; *Acc. Chem. Res.* **1988**, *21*, 114.

(5) Broderick, W. E.; Thomson, J. A.; Day, E. P.; Hoffman, B. M. *Science* **1990**, *249*, 401.

(6) Kahn, O.; Pei, Y.; Verdaguer, M.; Renard, J. P.; Sletten, J. *J. Am. Chem. Soc.* **1988**, *110*, 782.

(7) Nakatani, K.; Carriat, J. Y.; Journaux, Y.; Kahn, O.; Lloret, F.; Renard, J. P.; Pei, Y.; Sletten, J.; Verdaguer, M. *J. Am. Chem. Soc.* **1989**, *111*, 5739.

(8) Nakatani, K.; Bergerat, P.; Codjovi, E.; Mathonière, C.; Pei, Y.; Kahn, O. *Inorg. Chem.* **1991**, *30*, 3977.

(9) Pei, Y.; Kahn, O.; Nakatani, K.; Codjovi, E.; Mathonière, C.; Sletten, J. *J. Am. Chem. Soc.* **1991**, *113*, 6558.

(10) Caneschi, A.; Gatteschi, D.; Renard, J. P.; Rey, P.; Sessoli, R. *Inorg. Chem.* **1988**, *27*, 1756.

(11) Caneschi, A.; Gatteschi, D.; Sessoli, R.; Rey, P. *Acc. Chem. Res.* **1989**, *22*, 392.

(12) Caneschi, A.; Gatteschi, D.; Renard, J. P.; Rey, P.; Sessoli, R. *Inorg. Chem.* **1989**, *28*, 1676; **1989**, *28*, 2940.

(13) Zhong, Z. J.; Matsumoto, N.; Okawa, H.; Kida, S. *Chem. Lett.* **1990**, 87.

(14) Matsumoto, N.; Sakamoto, M.; Tamaki, H.; Okawa, H.; Kida, S. *Chem. Lett.* **1990**, 853.

(15) Iwamura, H. *Adv. Phys. Org. Chem.* **1990**, *26*, 179.

(16) Fujita, I.; Teki, Y.; Takui, T.; Kinoshita, T.; Itoh, K.; Miko, F.; Sewaki, Y.; Iwamura, H.; Izuoka, A.; Sagawara, T. *J. Am. Chem. Soc.* **1990**, *112*, 4074.

(17) Caneschi, A.; Gatteschi, D.; Laugier, J.; Rey, P.; Sessoli, R.; Zanchini, C. *J. Am. Chem. Soc.* **1988**, *110*, 2795.

(18) Boyd, P. D. W.; Li, Q.; Vincent, J. B.; Folting, K.; Chang, H. R.; Streib, W. E.; Huffman, J. C.; Christou, G.; Hendrickson, D. N. *J. Am. Chem. Soc.* **1988**, *110*, 8537.

0020-1669/92/1331-0625\$03.00/0 © 1992 American Chemical Society

spin structures involving both ferro- and antiferromagnetic couplings, as well as possibly cantings. Those situations i–iv are represented in I–IV in the form of two-dimensional arrays of spins.

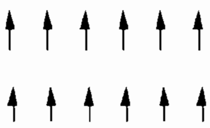

I

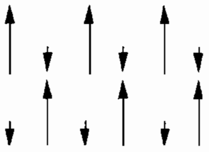

II

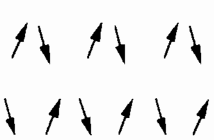

III

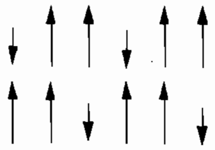

IV

It should be noticed, however, that in most of the cases the onset of a spontaneous magnetization results from a three-dimensional transition. In no case can it result from a one-dimensional ordering.

Situations I and II have been well documented in the last 4 years.[2–12] On the other hand, situation III has not been much investigated. Perhaps the best example of spin canting in molecular chemistry is provided by the β-polymorph of manganese(II) phthalocyanine (MnPc) with $T_c = 8.6$ K. The magnetic moment on a MnPc molecule is aligned perpendicularly to the molecular plane, reflecting the strong local anisotropy; the ferromagnetically coupled spins on a chain are almost perpendicular to those on the neighboring chain, resulting in a canted ferromagnetism.[19–25] Another very interesting example of weak ferromagnetism concerns the $FePS_3$ layered compound in which a mixture of pyridine and pyridinium is intercalated. Pure $FePS_3$ behaves as a two-dimensional antiferromagnet with a Neêl temperature of 120 K. The intercalated compound shows a weak ferromagnetic transition at $T_c = 90$ K.[26] Another interesting case of weak ferromagnetism in a Co(II) compound has recently been reported.[27]

In this paper we report on the unusual magnetic properties of the compound $Cu(ta)(3\text{-pic})\cdot H_2O$ (**2**) with ta = terephthalato and 3-pic = 3-picoline, which shows a weak ferromagnetic transition at $T_c = 2.8$ K. The crystal structure of **2** is not known, but that of its precursor $Cu(ta)(3\text{-pic})_2\cdot 0.5(3\text{-pic})\cdot 0.5CH_3OH$ (**1**) has been solved. Magnetic susceptibility measurements together with EPR spectra and low-field and high-field magnetization data lead to a satisfactory rationalization of the magnetic behavior.

Experimental Section

Syntheses. $Cu(ta)(3\text{-pic})_2\cdot 0.5(3\text{-pic})\cdot 0.5CH_3OH$ (**1**) was obtained in the form of medium blue prismatic type single crystals by slow diffusion of equimolecular (10^{-4} mol) amounts of piperidinium terephthalate and copper(II) acetate from a 1:1 solution mixture of methanol and 3-picoline. Those crystals are very fragile and evolve spontaneously and irreversibly in air to afford $Cu(ta)(3\text{-pic})\cdot H_2O$ (**2**). The transformation of **1** into **2** can also be achieved by treating **1** at room temperature with a methanolic solution containing one drop of water. **2** is more easily synthesized as follows: To 15 mL of a methanolic solution containing 338 mg (10^{-3} mol) of piperidinium terephthalate was added dropwise and under continuous stirring 50 mL of a 3-picolinic solution containing 200 mg (10^{-3} mol) of copper(II) acetate. The light blue microcrystalline material derived was left stirring for a while, filtered out, washed with methanol, and dried under vacuum. Anal. Calcd for $C_{14}H_{13}NO_5Cu$: C, 49.63; H, 3.87; N, 4.14; O, 23.61; Cu, 18.75. Found: C, 49.83; H, 3.77; N, 4.20; O, 22.90; Cu, 19.11.

Table I. Crystallographic Data for $Cu(ta)(3\text{-pic})_2\cdot 0.5(3\text{-pic})\cdot 0.5CH_3OH$

formula	$CuO_4N_2C_{20}H_{18}\cdot$ $0.5C_6NH_7\cdot 0.5OCH_4$	V, Å^3	2296 (26)
		Z	4
fw	475.5	μ(Mo Kα), cm^{-1}	9.8
space group	$P2_1/c$	d_{calc}, g cm^{-3}	1.37
a, Å	9.703 (4)	T	20 °C
b, Å	13.184 (8)	abs corr	DIFABS
c, Å	19.825 (4)	R^a	0.0449
β, deg	115.12 (2)	$R_w{}^a$	0.0469

[a] R and R_w are defined as follows: $R = \sum(|F_o| - |F_c|)/\sum|F_o|$; $R_w = [\sum w(|F_o| - |F_c|)^2/\sum F_o{}^2]^{1/2}$, with $w = 4F_o{}^2/\sigma^2(F_o{}^2)$.

Crystallographic Data Collection and Structure Determination. A selected crystal was inserted in a Lindemann glass tube together with a drop of a 1:1 methanol/3-picoline solvent mixture and set up on an Enraf-Nonius CAD4 diffractometer. Unit cell dimensions and the crystal orientation matrix together with their estimated standard deviations were obtained from least-squares refinements of the setting angles of 25 reflections. Two standard reflections were monitored periodically; the compound was very sensitive to X-rays, since at the end of data collection it had decayed by about 80%. Corrections were made by Lorentz and polarization effects and for decay. Empirical absorption corrections were applied (DIFABS).[28] Crystallographic data and other pertinent information are summarized in Table I. Computations were performed by using CRYSTALS[29] adapted on a MicroVax II computer. Atomic form factors for neutral Cu, O, C, N, and H were taken from ref 30. Anomalous dispersion was taken into account. No secondary extinction was observed. The structure was solved by interpretation of Patterson maps which clearly indicated the Cu atom position. All remaining non-hydrogen atoms were found by successive electron density map calculations. Their atomic coordinates were refined together with isotropic temperature factors. At this point residual peaks showed up close to inversion centers $^1/_2$, 0, $^1/_2$ and $^1/_2$, $^1/_2$, 0. They are compatible with 3-picoline in 0.5 statistical occupancy. The pyridine ring was treated as a six carbon atom ring with the same isotropic thermal vibration factor and a C–C distance constrained to 1.40 (1) Å. A subsequent Fourier series localized the methyl group, the position of which was refined without constraint. Other residual peaks appeared close to inversion centers 0, 0, $^1/_2$ and 0, $^1/_2$, 0. They were refined as a half-molecule of methanol in statistical distribution; methanol was indeed used as solvent during the synthesis. Atomic coordinates were refined with anisotropic temperature factors for the nondisordered part. At this stage, hydrogen atoms were located on a difference electron density map; their coordinates were refined with an overall isotropic temperature factor. Least-squares refinements were carried out by minimizing the function $\sum w(|F_o| - |F_c|)^2$, where F_o and F_c are observed and calculated structure factors. Models reached convergence with $R = \sum(\|F_o| - |F_c\|)/\sum|F_o|$ and $R_w = [\sum w(|F_o| - |F_c|)^2/\sum w(F_o)^2]^{1/2}$ values listed in Table I. Criteria for a satisfactory complete analysis were the ratios of the root-mean-square shift to standard deviation being less than 0.2 and no significant feature in the final difference maps. Atomic coordinates are given in Table II. Selected bond distances and bond angles are given in Table III.

Magnetic Susceptibility Measurements. These were carried out with two instruments, namely (i) a Faraday-type magnetometer equipped with a helium continuous-flow cryostat in the 4.2–300 K temperature range and (ii) a Mêtronique Ingéniêrie SQUID magnetometer working down to 1.5 K. This magnetometer can be used in low field (a few G) as well as in high field (up to 8 T). Diamagnetic corrections were estimated as -200×10^{-6} cm^3 mol^{-1} for **1** and -160×10^{-6} cm^3 mol^{-1} for **2**.

Magnetization Measurements. The low-field magnetization measurements were carried out with the SQUID magnetometer described above. The high-field measurements were performed at the "Service National des Champs Intenses" by means of a fluxmetric method. The sample was extracted in a constant magnetic field between compensated

---

(19) Lever, A. B. P. *J. Chem. Soc.* **1965**, 1821.
(20) Barraclough, C. G.; Martin, R. L.; Mitra, S. *J. Chem. Phys.* **1970**, *53*, 1638.
(21) Barraclough, C. G.; Gregson, A. K.; Mitra, S. *J. Chem. Phys.* **1974**, *60*, 962.
(22) Mioyoshi, H.; Ohya-Nishiguchi, H.; Deguchi, Y. *Bull. Chem. Soc. Jpn.* **1973**, *46*, 2724. Miyoshi, H. *Bull. Chem. Soc. Jpn.* **1974**, *47*, 561; *J. Phys. Soc. Jpn.* **1974**, *37*, 50.
(23) Figgis, B. N.; Williams, G. A.; Forsyth, J. B.; Mason, R. *J. Chem. Soc., Dalton Trans.* **1981**, 1837.
(24) Mitra, S.; Gregson, A. K.; Hatfield, W. E.; Weller, R. R. *Inorg. Chem.* **1983**, *22*, 1729.
(25) Awaga, K.; Maruyama, Y. *Phys. Rev. B* **1991**, *44*, 2589.
(26) Clement, R.; Lomas, L.; Audière, J. P. *Chem. Mater.* **1990**, *2*, 641.
(27) Moron, M. C.; Palacio, F.; Pons, J.; Casabo, J.; Carlin, R. L. *Eur. J. Solid State Inorg. Chem.* **1991**, *28*, 431.
(28) Walker, N.; Stuart, D. *Acta Crystallogr., Sect. A* **1983**, *A34*, 159.
(29) Watkin, D. J.; Carruthers, J. R.; Betteridge, P. W. CRYSTALS, an Advanced Crystallographic Program System. Chemical Crystallography Laboratory, University of Oxford, Oxford, U.K., 1988.
(30) Cromer, D. T.; Waber, J. T. In *International Tables for X-Ray Crystallography*; Kynoch Press: Birmingham, U.K., 1974; Vol. IV, p 99, Table 2.2B.

Table II. Fractional Atomic Coordinates with Esd's in Parentheses and *U* for Cu(ta)(3-pic)$_2$·0.5(3-pic)·0.5CH_3OH

atom	*x*/*a*	*y*/*b*	*z*/*c*	U_{iso}	U_{eq}[a]
Cu	0.89732 (9)	0.35655 (7)	0.44375 (4)		0.0328
O(1)	0.7066 (5)	0.3432 (5)	0.3507 (2)		0.0363
C(1)	0.6994 (8)	0.2513 (7)	0.3324 (4)		0.0268
O(2)	0.7978 (6)	0.1878 (4)	0.3675 (3)		0.0473
C(2)	0.5596 (7)	0.2200 (6)	0.2642 (4)		0.0276
C(3)	0.4509 (8)	0.2880 (6)	0.2219 (4)		0.0361
C(4)	0.3257 (8)	0.2566 (6)	0.1583 (4)		0.0279
C(5)	0.3097 (7)	0.1557 (7)	0.1373 (3)		0.0258
C(6)	0.4167 (7)	0.0858 (6)	0.1811 (4)		0.0345
C(7)	0.5402 (7)	0.1193 (6)	0.2435 (4)		0.0316
C(8)	0.1792 (8)	0.1188 (6)	0.0674 (4)		0.0238
O(3)	0.1721 (5)	0.0289 (4)	0.0507 (3)		0.0400
O(4)	0.0817 (5)	0.1853 (4)	0.0291 (2)		0.0369
N(1)	1.0143 (7)	0.3902 (5)	0.3837 (3)		0.0410
C(10)	0.9779 (9)	0.4715 (7)	0.3393 (4)		0.0446
C(11)	1.055 (1)	0.5045 (8)	0.2986 (5)		0.0638
C(12)	1.175 (1)	0.445 (1)	0.3043 (6)		0.0776
C(13)	1.213 (1)	0.363 (1)	0.3483 (6)		0.0930
C(14)	1.131 (1)	0.3355 (8)	0.3880 (4)		0.0662
C(15)	1.006 (2)	0.5947 (9)	0.2499 (6)		0.0923
N(2)	0.7781 (6)	0.3254 (5)	0.5038 (3)		0.0314
C(16)	0.8228 (7)	0.2556 (6)	0.5569 (4)		0.0400
C(17)	0.7448 (9)	0.2295 (6)	0.5986 (4)		0.0418
C(18)	0.613 (1)	0.2827 (7)	0.5834 (5)		0.0573
C(19)	0.5645 (9)	0.3538 (7)	0.5294 (5)		0.0551
C(20)	0.6478 (8)	0.3739 (6)	0.4900 (4)		0.0499
C(21)	0.803 (1)	0.1487 (8)	0.6588 (5)		0.0691
O(30)	−0.106 (2)	0.513 (1)	−0.1057 (8)	0.1200	
C(30)	−0.003 (3)	0.468 (2)	−0.032 (1)	0.1200	
C(31)	0.584 (3)	0.525 (3)	−0.011 (2)	0.123 (3)	
C(32)	0.570 (3)	0.467 (2)	−0.072 (1)	0.123 (3)	
C(33)	0.443 (3)	0.402 (2)	−0.099 (1)	0.123 (3)	
C(34)	0.359 (3)	0.379 (2)	−0.058 (1)	0.123 (3)	
C(35)	0.363 (3)	0.446 (2)	−0.003 (2)	0.123 (3)	
C(36)	0.485 (3)	0.515 (2)	0.024 (1)	0.123 (3)	
C(37)	0.503 (3)	0.600 (3)	0.076 (2)	0.123 (3)	

[a] $U_{eq} = (U_1U_2U_3)^{1/3}$.

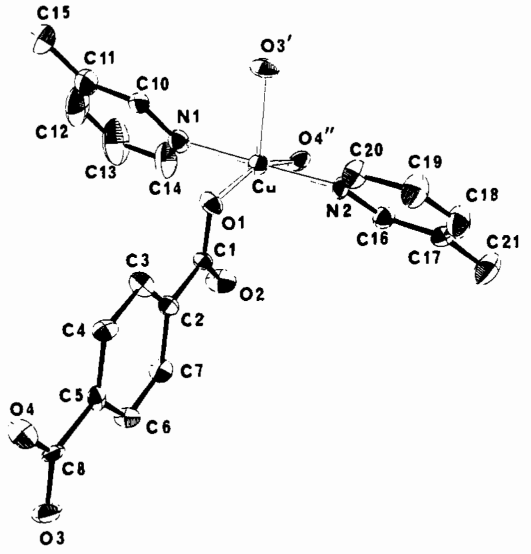

Figure 1. Perspective view of the Cu(ta)(3-pic)$_2$ unit in **1**, showing the labeling scheme. Single and double primes as superscripts refer to the following equivalent positions relative to the *x*, *y*, *z* sets: (′) $1 - x$, $^1/_2 + y$, $^1/_2 - z$; (″) $1 + x$, $^1/_2 - y$, $^1/_2 + z$.

pick-up coils connected in series opposition. The integrated signal of the induced voltage was proportional to the magnetization. The continuous magnetic field up to 20 T was produced by a water-cooled Bitter magnet. The calibration and the sensitivity of the apparatus was previously described in detail.[31] The results are expressed in $N\beta$ (or Bohr magnetons per mole) units. It is recalled that $N\beta$ = 5583 cm^3 G mol^{-1}.

Table III. Selected Interatomic Distances (Å) and Bond Angles (deg) with Esd's in Parentheses for Cu(ta)(3-pic)$_2$·0.5(3-pic)·0.5CH_3OH[a]

Cu–O(1)	1.990 (4)	Cu–N(1)	2.012 (6)
Cu–O(3′)	2.386 (6)	Cu–N(2)	2.023 (5)
Cu–O(4″)	1.949 (4)		
O(1)–C(1)	1.258 (8)	O(3)–C(8)	1.223 (8)
O(2)–C(1)	1.238 (8)	O(4)–C(8)	1.278 (8)
C(1)–C(2)	1.51 (1)	C(4)–C(5)	1.38 (1)
C(2)–C(3)	1.368 (9)	C(5)–C(6)	1.38 (1)
C(2)–C(7)	1.38 (1)	C(5)–C(8)	1.506 (9)
C(3)–C(4)	1.39 (1)	C(6)–C(7)	1.379 (9)
N(1)–C(10)	1.34 (1)	N(2)–C(16)	1.325 (9)
N(1)–C(14)	1.32 (1)	N(2)–C(20)	1.337 (9)
C(10)–C(11)	1.38 (1)	C(16)–C(17)	1.38 (1)
C(11)–C(12)	1.37 (1)	C(17)–C(18)	1.37 (1)
C(11)–C(15)	1.48 (1)	C(17)–C(21)	1.52 (1)
C(12)–C(13)	1.339 (9)	C(18)–C(19)	1.35 (1)
C(13)–C(14)	1.38 (1)	C(19)–C(20)	1.37 (1)
Cu···Cu‴	4.414 (2)		
O(1)–Cu–O(3′)	87.6 (2)	O(3′)–Cu–N(1)	93.3 (2)
O(1)–Cu–O(4″)	158.3 (3)	O(3′)–Cu–N(2)	85.6 (2)
O(1)–Cu–N(1)	90.4 (2)	O(4″)–Cu–N(1)	92.0 (2)
O(1)–Cu–N(2)	89.3 (2)	O(4″)–Cu–N(2)	88.6 (2)
O(3′)–Cu–O(4″)	113.8 (2)	N(1)–Cu–N(2)	178.9 (3)
O(1)–C(1)–O(2)	123.7 (7)	C(4)–C(5)–C(6)	119.5 (6)
O(1)–C(1)–C(2)	116.1 (7)	C(4)–C(5)–C(8)	112.1 (7)
O(2)–C(1)–C(2)	120.2 (8)	C(6)–C(5)–C(8)	118.4 (8)
C(1)–C(2)–C(3)	122.4 (8)	C(5)–C(6)–C(7)	119.0 (7)
C(1)–C(2)–C(7)	119.2 (7)	C(2)–C(7)–C(6)	122.2 (6)
C(3)–C(2)–C(7)	118.4 (6)	O(3)–C(8)–O(4)	124.1 (7)
C(2)–C(3)–C(4)	120.7 (8)	O(3)–C(8)–C(5)	119.4 (7)
C(3)–C(4)–C(5)	120.2 (7)	O(4)–C(8)–C(5)	116.5 (7)
C(10)–N(1)–C(14)	117.5 (7)	C(16)–N(2)–C(20)	117.2 (6)
N(1)–C(10)–C(11)	125.5 (9)	N(2)–C(16)–C(17)	124.8 (7)
C(10)–C(11)–C(12)	115.2 (9)	C(16)–C(17)–C(18)	115.8 (7)
C(10)–C(11)–C(15)	122.3 (11)	C(16)–C(17)–C(21)	121.9 (7)
C(12)–C(11)–C(15)	122.5 (11)	C(18)–C(17)–C(21)	122.4 (8)
C(11)–C(12)–C(13)	120.0 (10)	C(17)–C(18)–C(19)	120.8 (8)
C(12)–C(13)–C(14)	121.4 (10)	C(18)–C(19)–C(20)	119.5 (7)
N(1)–C(14)–C(13)	120.4 (9)	N(2)–C(20)–C(19)	121.9 (7)

[a] Single, double, and triple primes as superscripts refer to the following equivalent positions relative to the *x*, *y*, *z* set: (′) $1 - x$, $0.5 + y$, $0.5 - z$; (″) $1 + x$, $0.5 - y$, $0.5 + z$; (‴) $2 - x$, $1 - y$, $1 - z$.

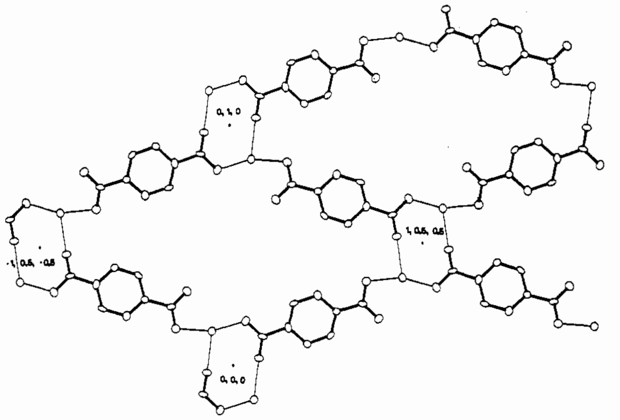

Figure 2. Packing diagram projected down to the chain plane for **1**.

EPR Spectra. The X-band powder EPR spectra were recorded at various temperatures between 4.2 and 300 K with an ER 200D Bruker spectrometer equipped with a helium continuous-flow cryostat and a Hall probe.

Description of the Structure of Cu(ta)(3-pic)$_2$·0.5(3-pic)·0.5CH_3OH (1)

The structure consists of Cu(ta)(3-pic)$_2$ complex units bound together so that the [Cu(ta)]$_n$ skeleton forms an infinite layer to which the 3-pic molecules are perpendicular and noncoordinated 3-pic and CH_3OH molecules. One of the units is shown in Figure 1 together with the atom-numbering scheme. The copper(II) ion

---

(31) Picoche, J.; Guillot, M.; Marchand, A. *Physica* **1989**, *B155*, 407.

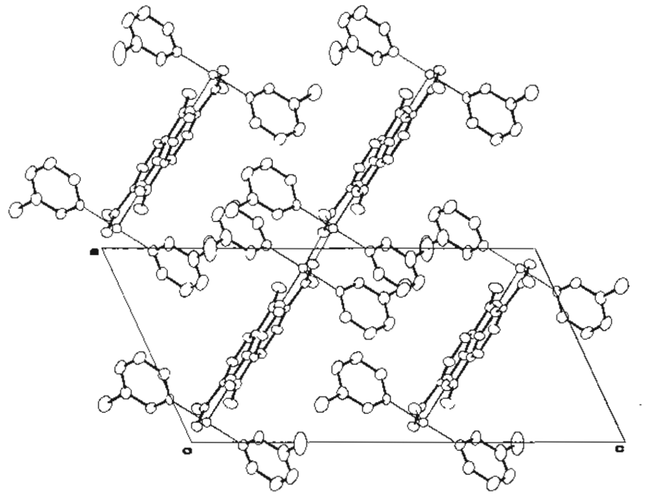

Figure 3. Packing diagram projected down to the *b* axis for **1**. The 3-picoline and methanol noncoordinated molecules are omitted for clarity.

is in a 4 + 1 distorted square-pyramidal environment. Basal plane positions are occupied by two trans nitrogen atoms of 3-picoline molecules and two oxygen atoms O(1) and O(4″) (1 + *x*, $^1/_2$ − *y*, $^1/_2$ + *z*) belonging to two terephthalate groups. The apical position is occupied by the O(3′) (1 − *x*, $^1/_2$ + *y*, $^1/_2$ − *z*) oxygen atom of a third terephthalate group.

In the lattice, the $Cu(ta)(3\text{-}pic)_2$ units are centrosymmetrically associated with respect to inversion centers 0, 0, 0 and 0, $^1/_2$, $^1/_2$, as shown in Figure 2, affording copper(II) pairs with a Cu⋯Cu separation of 4.414 Å. All the other Cu⋯Cu separations are larger than 9 Å. The Cu⋯Cu separations through the terephthalate bridge are equal to 10.566 and 10.892 Å.

Each terephthalate is bound to three copper atoms. One of the two carboxylate groups bridges two copper atoms to form the pair described above with a short Cu–O(4) = 1.949 Å and a long Cu–O(3) = 2.386 Å bond lengths. The other carboxylate group is monocoordinated with a short Cu–O(1) = 1.990 Å bond length, the separation between the copper atom and the second oxygen atom of this carboxylate being Cu–O(2) = 2.632 Å. The copper(II) pairs are linked together through the terephthalate bridges so that they form an infinite bidimensional layer. Four terephthalate groups lie along the edges of a parallelogram, a diagonal of which is parallel to the *b* axis. The crystal is made of such layers approximately perpendicular to the *ac* plane. 3-Picoline molecules, coordinated or not, fill the space between layers as shown in Figure 3.

The coordination of 2-picoline to copper(II) has been reported in $Cu(2\text{-}pic)_2X_2$, compounds which adopt a monomeric structure due to steric hindrances on behalf of the methyl groups of the two 2-picoline molecules.[32] On the contrary, the methyl groups of the two 3-picoline molecules coordinated to the same metal ion in **1** are aligned on opposite sides of the pic–Cu–pic direction, thus facilitating the polymeric structure. To complete this section concerning the structure of **1**, we can mention that the same kind of structure should be obtained if 3-picoline was replaced by pyridine or 4-picoline. The structure was refined with the 3-picoline derivative because it gives the best shaped single crystals.

Magnetic and EPR Properties

$Cu(ta)(3\text{-}pic)_2\cdot 0.5(3\text{-}pic)\cdot 0.5CH_3OH$. The magnetic behavior of $Cu(ta)(3\text{-}pic)_2\cdot 0.5(3\text{-}pic)\cdot 0.5CH_3OH$ is quite simple. The molar magnetic susceptibility χ_M follows the Curie law in the whole 4.2 ≤ T/K ≤ 300 temperature range with a $\chi_M T$ value of 0.40 cm^3 K, as expected for a noncoupled copper(II) compound. The EPR spectrum is also typical of isolated copper(II) in elongated tetragonal environment with $g_x = g_y = 2.07$ and $g_z = 2.18$. These findings indicate that the copper(II) ions interact neither through the terephthalate bridges nor within the pairs described in the previous section. This situation can be rather easily explained. The unpaired electron coming from the copper(II) ion occupies a d-type magnetic orbital pointing toward the four nearest neighbors in the basal plane, i.e. the O(1), O(4″), N(1), and N(2) atoms. This orbital is roughly perpendicular to both the plane of the terephthalate bridge and that of the bridging network within the pair. It has been proved that the coplanarity of the terephthalate and of the magnetic orbital was a prerequisite to observe an interaction through this bridge between two magnetic centers far apart from each other.[33] As far as the copper(II) pair is concerned, the two centrosymmetrically related magnetic orbitals are also unfavorably oriented to interact. Indeed, each of them is delocalized toward the O(4″) atom of the bridging network but not on the O(3′) atom occupying the apical position. It follows that these orbitals cannot overlap as schematized in Figure 4. The key role in this behavior is played by the two 3-picoline molecules coordinated on both sides of the $[Cu(ta)]_n$ layer. These molecules

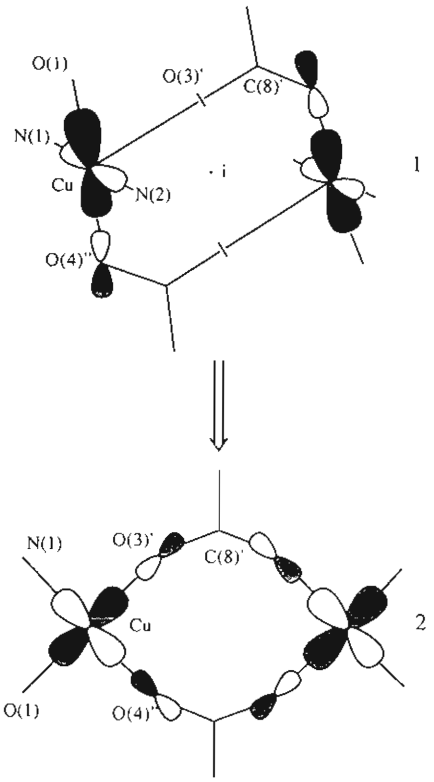

Figure 4. Proposed structure of the copper(II) pair in **2** and orientations of the magnetic orbitals within such a pair in **1** and **2**.

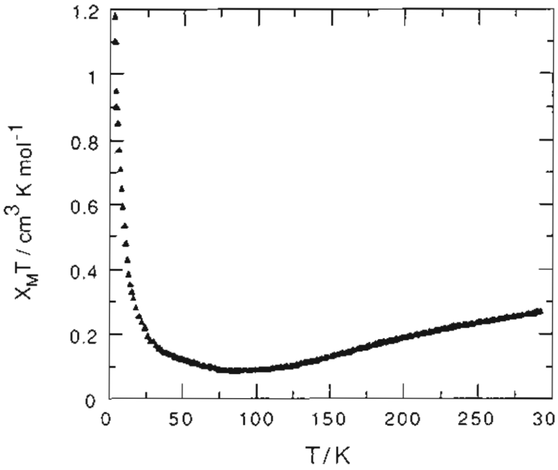

Figure 5. $\chi_M T$ versus T plot for **2**.

---

(32) Cameron, A. F.; Taylor, D. W.; Nutall, R. H. *J. Chem. Soc., Dalton Trans.* **1972**, 58.

(33) Chandhuri, P.; Oder, K.; Wieghardt, K.; Gehring, S.; Haase, W.; Nuber, B.; Weiss, J. *J. Am. Chem. Soc.* **1988**, *110*, 3657.

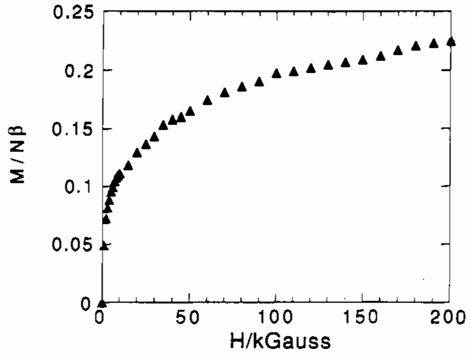

Figure 6. Field dependence up to 20 T of the magnetization for **2**.

provoke a reversal of the magnetic orbitals[34] as compared to what the situation would be if the basal plane of the copper(II) ion was within the layer and not perpendicular to it.

Cu(ta)(3-pic)(H_2O). This compound exhibits a kind of magnetic behavior which is quite exceptional in molecular chemistry. The $\chi_M T$ versus T plot within a field of 0.2 T is shown in Figure 5. At room temperature, $\chi_M T$ is equal to 0.269 (5) cm^3 K mol^{-1}, which is already weaker than expected for a noncoupled copper(II) compound ($N\beta^2 g^2/4k \approx 0.40$ cm^3 K mol^{-1}). When the temperature is lowered, $\chi_M T$ first decreases, reaches a minimum around 85 K with $\chi_M T = 0.088$ (5), and then increases more and more rapidly. $\chi_M T$ reaches 0.90 cm^3 K mol^{-1} at 4.2 K and 1.20 cm^3 K mol^{-1} at 3 K. This last value is about three times as large as expected for a noncoupled copper(II) species. To sum up, the molar magnetic susceptibility is weaker than that of an isolated copper(II) compound above 85 K, which suggests some antiferromagnetic interaction, and higher than that of this hypothetical isolated copper(II) compound below 85 K, which is reminiscent of some ferromagnetic interaction.

To get more information on **2**, we investigated the variation of the magnetization M versus the applied magnetic field H in the field range $0 \leq H/\mathrm{T} \leq 20$ and at 1.3 K. The results are shown in Figure 6. The two main features of this magnetization study are the following: (i) the zero-field magnetic susceptibility $(dM/dH)_{H=0}$ is much higher than expected for a compound containing isolated copper(II) ions; (ii) even at very high field (20 T) the magnetization does not reach the saturation value expected for a copper(II) compound, i.e. $N\beta g/2$ (≈ 1.05 $N\beta$). Actually, M continuously increases when the field increases, the M versus H plot being linear above ca. 8 T, and is equal to only 0.225 $N\beta$ at 20 T. This indicates that even a field of 20 T is far from being sufficient to align all the local spins along the direction of the field.

The third type of magnetic experiment we carried out consisted in measuring the field-cooled magnetization (FCM) and the zero-field-cooled magnetization (ZFCM) in the 1.6–6 K temperature range. The FCM obtained in cooling the sample within a field of 5 G shows a rapid increase below 4 K. The ZFCM obtained in cooling the sample in zero field and then warming it within the field of 5 G is weaker than the FCM below 2.8 K. The difference FCM − ZFCM corresponds to the remnant magnetization induced in cooling within the field below 2.8 and switching off the field. This remnant magnetization vanishes upon warming at 2.8 K. Those data shown in Figure 7 indicate that the compound exhibits a zero-field magnetization below a critical temperature $T_c = 2.8$ K.

The X-band powder EPR spectrum of **2** shown in Figure 8 is also very informative. This spectrum presents four well-resolved features at 950, 4590, 5687, and 6990 G belonging to the actual compound in addition to a sharp feature at 3254 G most likely due to a noncoupled copper(II) impurity. We checked that no other feature was detected up to 12×10^3 G. When the temperature is lowered, the absolute intensities of all the features but that at 3254 G diminish, and the spectrum vanishes below 80 K.

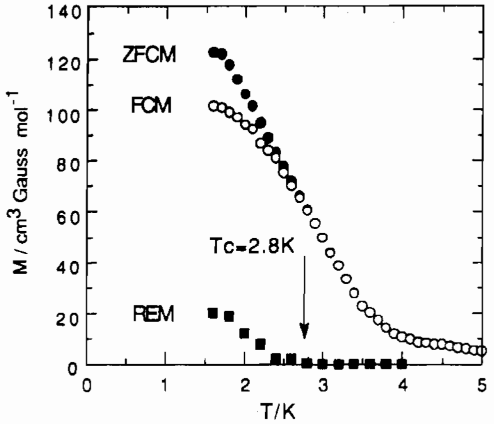

Figure 7. Temperature dependence of the magnetization for **2** within a field of 5 G: (○) FCM; (●) ZFCM; (■) REM.

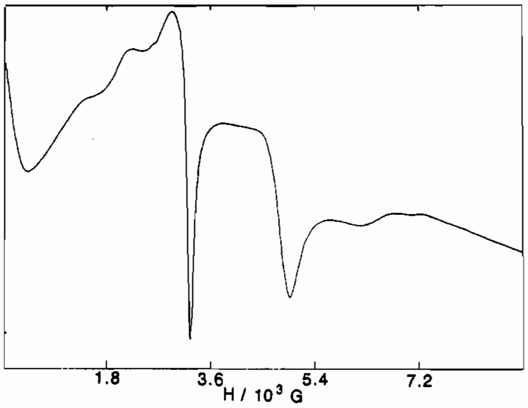

Figure 8. X-Band powder EPR spectrum for **2** at 300 K.

The shape and the temperature dependence of this spectrum are quite typical of an excited triplet pair state,[35] the four features corresponding to the H_{z1}, H_{x2}, H_{y2}, and H_{z2} resonances in the case where the axial zero-field-splitting parameter D is larger than the value of the incident quantum (≈ 0.3 cm^{-1}). To interpret this spectrum quantitatively, we assumed that Wasserman's equations were valid, i.e. that the zero-field-splitting **D** and Zeeman **g** tensors were coaxial.[36] If so, an excellent agreement is obtained between observed and calculated resonant fields with $g_x = g_y = 2.00$, $g_z = 2.22$, $|D| = 0.414$ cm^{-1}, and $E = 0.028$ cm^{-1}. We recall that $D = 3D_{zz}/2$ and $E = (D_{xx} - D_{yy})/2$. The spectrum also shows a poorly resolved feature around 1700 G, the origin of which is not understood yet.

Discussion

This section will be entirely devoted to the interpretation of the magnetic data concerning Cu(ta)(3-pic)·H_2O (**2**). The EPR spectrum reveals an excited spin triplet pair state fully depopulated below 80 K. The crystal structure of **2** is not known, and the chances of growing single crystals suitable for X-ray diffraction seem very low. However, this structure should be reminiscent of that of the precursor **1**, the structure of which actually shows copper(II) pairs with a Cu···Cu separation of 4.414 Å. It is therefore legitimate to postulate that those pairs do also exist in **2**. In **1**, the copper(II) ions within a pair are noncoupled owing to unfavorable orientations of the magnetic orbitals. In **2**, on the other hand, they are antiferromagnetically coupled with a large singlet–triplet energy gap J. This is possible if the two magnetic orbitals instead of being perpendicular to are localized within the bridging network $Cu(OCO)_2Cu$. The condition in order for such a situation to be realized is that the basal planes around the copper

---

(34) Girerd, J. J.; Kahn, O.; Verdaguer, M. *Inorg. Chem.* **1980**, *19*, 274.

(35) Bencini, A.; Gatteschi, D. *EPR of Exchange Systems*; Springer-Verlag: Berlin, 1990.

(36) Wasserman, E.; Snyder, L. C.; Yager, W. A. *J. Chem. Phys.* **1964**, *41*, 1763.

atoms and the bridging network are (quasi) coplanar.[37] A possible structure fulfilling this condition is schematized in Figure 4. The four nearest neighbors of a copper atom are O(1) belonging to a monodentate terminal carboxylate, the nitrogen atom N(1) or N(2) of a 3-picoline molecule, O(3′) belonging to one of the two bridging carboxylates, and O(4″) belonging to another bridging carboxylate. As discussed further, this pair is certainly not centrosymmetric. An alternative structure would be that where the two peripheral nearest neighbors of a copper atom would be O(1) and O(2) belonging both to a terminal carboxylate group. The 3-picoline molecule would then occupy an apical position. This latter hypothesis seems to us less probable. Indeed, when oxygen and nitrogen atoms are in competition as nearest neighbors, copper(II) most often chooses a nitrogen atom.[37] The key point in the mechanism we propose is that the Cu–O(3′) bond is long in **1** (2.632 Å) and short in **2**. Such a structural transformation involving only small displacements may certainly occur in the solid state. It is obviously favored by the plasticity of the copper(II) coordination sphere.[38]

The magnetic susceptibility data in the 85–300 K temperature range at first view seem to be consistent with such a pair structure. $\chi_M T$ rapidly decreases when T decreases, which is in line with a large intrapair antiferromagnetic interaction. Those data can be reasonably well fitted with the Bleaney–Bowers pair law.[39] The singlet–triplet energy gap is found to be of the order of $J = -330$ cm^{-1}. However, for a genuine pair compound with a singlet ground state well separated in energy from the triplet excited state, $\chi_M T$ is expected to tend to zero, or to a very weak value if some noncoupled impurity is present, when T approaches absolute zero. Moreover, the magnetization at 4.2 K should be zero, since at this temperature the excited magnetic state is totally depopulated. We have seen in the preceding section that experimental susceptibility and magnetization data do not follow such behaviors. Even in the temperature range where the triplet state is depopulated, **2** does not behave as a diamagnetic material. In fact the data reveal a ferromagnetic behavior below 85 K and a zero-field magnetization below 2.8 K. These findings indicate that the ground pair state is not a pure singlet state but contains some proportion of a magnetic state. There is a well-known mechanism coupling singlet and triplet states in a copper(II) pair, namely the antisymmetric interaction phenomenologically described by the term $d \cdot S_A \wedge S_B$ occurring in the zero-field spin Hamiltonian:[40–44]

$$H = -J S_A \cdot S_B + S_A \cdot \mathbf{D}_{AB} \cdot S_B + \vec{d} \cdot S_A \wedge S_B \qquad (1)$$

S_A and S_B are the local spin operators, $\mathbf{D}_{AB}$ is the tensor describing both the dipolar and anisotropic interactions, and $\vec{d}$ is a vector characterizing the antisymmetric interaction. Neglecting $\mathbf{D}_{AB}$ and assuming that J is negative and much larger than the components d_u ($u = x, y, z$) of $\vec{d}$ result in the spectrum of low-lying states shown as follows:

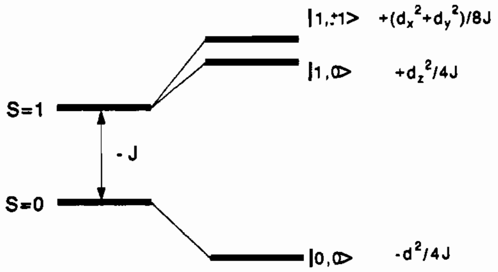

The wave function Ψ for this ground state is

$$\Psi = [1 - (d^2/4J^2)]^{-1/2}\Big\{|0,0\rangle - (2J)^{-1}\Big[\big(\sqrt{2}/2\big)(id_x + d_y)|1,1\rangle - id_z|1,0\rangle - \big(\sqrt{2}/2\big)(id_x - d_y)|1,-1\rangle\Big]\Big\} \qquad (2)$$

The antisymmetric interaction tends to orient the two local spins perpendicularly to each other, while the isotropic interaction tends to orientate them in antiparallel directions. It results in a canting angle α between these local spins in the state which otherwise would be diamagnetic, and the resulting spin is different from zero. To our knowledge, the presence of an antisymmetric interaction in antiferromagnetically coupled copper(II) pairs has not been demonstrated yet. Owing to the singlet–triplet mixing, the average magnetic suceptibility defined as

$$\chi_M = (\chi_x + \chi_y + \chi_z)/3 \qquad (3)$$

does not tend to zero when T approaches zero but to a low-temperature limit $(\chi_M)_{LT}$ given by

$$(\chi_M)_{LT} = -Ng^2\beta^2 d^2/3J^3 \qquad (4)$$

in the approximation where the local **g** tensor for the copper(II) ion is assumed to be isotropic with the principal value g. Since J is negative, $(\chi_M)_{LT}$ is positive. In the temperature range where only this ground state is thermally populated, the magnetic susceptibility is constant and given by (3). This effect is quite similar to temperature-independent paramagnetism (TIP).

The magnetic behavior of **2** does not correspond to this model yet. The copper(II) pairs are not isolated magnetically but are connected by terephthalate bridges able to transmit some interpair interaction. The actual situation may then be described as follows: Within the pairs, the copper(II) ions are coupled antiferromagnetically with, however, a nonzero magnetic moment in the ground state due to antisymmetric interaction. These residual pair magnetic moments couple ferromagnetically through the terephthalate bridges within the crystal lattice, as schematized:

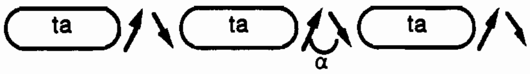

Below 2.8 K, all pair magnetic moments are oriented along the same direction so that **2** exhibits a zero-field magnetization. This type of weak ferromagnetism involving copper(II) pairs weakly coupled to each other through extended groups to the best of our knowledge has never been described yet.

The magnetization data allow one to estimate both the modulus of $\vec{d}$ and the canting angle α between two local spins within a pair. Indeed, we have

$$\sin \alpha = |d/J| \qquad (5)$$

$$\sin \alpha = M_0/M_S \qquad (6)$$

where M_0 is the intersect of the linear part of the M versus H plot with the M axis and M_S is the saturation magnetization. M_0 is found equal to 0.16 $N\beta$. It follows that α is equal to 8.5° and d to 48 cm^{-1}.

If the magnetic behavior of **2** seems to be rather well understood, at least two aspects deserve to be discussed further. The first problem concerns the crystal structure of **2**. The fact that we did not succeed in getting single crystals of **2** is obviously the weak point of this work. The EPR spectra clearly indicate that **2** contains copper(II) pairs. In contrast to what happens for **1**, however, those pairs are antiferromagnetically coupled ($J \approx -330$ cm^{-1}), which may be easily explained by a reversal of the magnetic orbitals. In addition, the antisymmetric interaction mixing ground singlet and excited triplet states operates. If so, the symmetry of the pairs is very low. The inversion center existing for **1** has disappeared.

The second problem deals with the mechanism of the interpair interactions through the terephthalate bridges. In the scheme above it is implicitly assumed that those interactions ferromagnetically align the residual magnetic moments arising from the

---

(37) Kahn, O. *Angew. Chem., Int. Ed. Engl.* **1985**, *24*, 834.
(38) Gazo, J.; Bersuker, I. B.; Garaj, J.; Kabesova, M.; Kohout, J.; Langfelderova, H.; Melnik, M.; Serator, M.; Valach, F. *Coord. Chem. Rev.* **1976**, *19*, 253.
(39) Bleaney, B.; Bowers, K. D. *Proc. R. Soc. London* **1952**, *A214*, 451.
(40) Dzyaloshinsky, I. *Sov. Phys. JETP* **1958**, *6*, 1130.
(41) Dzyaloshinsky, I. *J. Phys. Chem. Solids* **1958**, *4*, 241.
(42) Moriya, T. *Phys. Rev.* **1960**, *120*, 91.
(43) Erdös, P. *J. Phys. Chem. Solids* **1966**, *27*, 1705.
(44) Erdös, P. *Helv. Phys. Acta* **1966**, *39*, 155.

antisymmetric coupling within the copper(II) pairs. In principle, they could lead to a zero resulting magnetic moment as well. This canceling effect is schematized as

Right now, we do not see well the conditions which have to be fulfilled to favor one situation rather than another. We hope to be able to clarify this question in the near future.

As a conclusion, we want to point out that weak ferromagnetism in molecular chemistry deserves to be investigated in a thorough fashion. It might be also an interesting strategy to design molecular-based materials exhibiting a zero-field magnetization. This paper is one of the first ones focusing on this facet of molecular magnetism.

It is also worth emphasizing that, in most of the copper(II) terephthalate derivatives, the metal ions are magnetically isolated or very weakly coupled.[45,46] In one or two cases, owing to quite favorable orientations of the magnetic orbitals, a rather large antiferromagnetic interaction is detected.[33,47] In **2**, the terephthalate groups propagate a ferromagnetic interaction between residual pair magnetic moments. Another case of ferromagnetism in copper(II) terephthalate derivatives has been recently reported.[48]

Acknowledgment. E.B. thanks the EEC, which financially supported his stay in Orsay, France.

Supplementary Material Available: Tables of crystal data collection parameters and refinement conditions, anisotropic temperature factors, important least-squares planes, and hydrogen coordinates (5 pages); a table of observed and calculated structure factors (5 pages). Ordering information is given on any current masthead page.

---

(45) Verdaguer, M.; Gouteron, J.; Jeannin, S.; Jeannin, Y.; Kahn, O. *Inorg. Chem.* **1984**, *23*, 4291.

(46) Bakalbassis, E. G.; Mrozinski, J.; Tsipis, C. A. *Inorg. Chem.* **1986**, *25*, 3684.

(47) Bakalbassis, E. G.; Tsipis, C. A.; Mrozinski, J. *Inorg. Chem.* **1985**, *24*, 4291.

(48) Bakalbassis, E. G.; Kahn, O.; Bergerat, P.; Jeannin, S.; Jeannin, Y.; Dromzee, Y. *J. Chem. Soc., Chem. Commun.* **1990**, 1771.

Contribution from the Department of Chemistry, University of Newcastle, Callaghan, New South Wales 2308, Australia, and School of Chemistry, University of Sydney, New South Wales 2006, Australia

Platinum(IV) Complexes of a Tetraaza Macrocycle with Pendent Dichloroamine or Ammonium Groups

Paul V. Bernhardt,[1a] Geoffrey A. Lawrance,[*,1a] and Trevor W. Hambley[1b]

Received June 11, 1991

Reaction of the platinum(II) complex of the pendent-arm macrocycle 6,13-diammonio-6,13-dimethyl-1,4,8,11-tetraazacyclotetradecane with chlorine in aqueous solution does not lead simply to oxidation of the platinum(II) complex to a *trans*-dichloroplatinum(IV) complex. Instead, complete chlorination of the pendent primary amines occurs also, producing the *trans*-dichloroplatinum(IV) complex of a bis(dichloroamino) macrocycle. The dichloroamino complex was characterized by a crystal structure analysis, the first X-ray crystal structure of a dichloroamine; the perchlorate salt of *trans*-$[Pt(\mathbf{2})Cl_2](ClO_4)_2$ crystallized in the $P2_1/n$ space group, with $Z = 2$, $a = 10.612$ (5) Å, $b = 10.280$ (3) Å, $c = 12.792$ (4) Å, and $\beta = 110.56$ (3)°. Inequivalent N–Cl bond lengths (1.718 (12) and 1.779 (12) Å) were observed. In aqueous acid, slow dechlorination occurs to produce the *trans*-dichloroplatinum(IV) complex of the precursor macrocycle, also characterized by a crystal structure analysis. The complex of the precursor macrocycle, *trans*-$[Pt(\mathbf{1})Cl_2]Cl_2(ClO_4)_2\cdot 4H_2O$, crystallized in the $P\bar{1}$ space group, with $Z = 1$, $a = 7.308$ (2) Å, $b = 10.448$ (2) Å, $c = 10.672$ (2) Å, $\alpha = 103.89$ (1)°, $\beta = 104.50$ (1)°, and $\gamma = 103.90$ (1)°.

Although the syntheses and reactivities of chloroamine compounds have been well studied and reviewed,[2-4] structural studies of these compounds have been few. This paucity stems from the inherent instability of these compounds; in fact, many are explosive. An earlier paper[5] reported the syntheses and X-ray crystal structures of square-planar platinum(II) and palladium(II) complexes of the pendent-arm macrocycle 6,13-diammonio-6,13-dimethyl-1,4,8,11-tetraazacyclotetradecane (**1**). The platinum(II) complex of this macrocycle was reacted with chlorine in order to investigate the competition between the oxidant and the pendent primary amines for the axial coordination sites on going from square-planar (Pt^{II}) to octahedral (Pt^{IV}) geometry. The product was found to be a *trans*-dichloro(tetraamine)platinum(IV) complex, but chlorination of both pendent amines also occurred, resulting in the novel coordinated macrocycle (6,13-bis(dichloroamino)-6,13-dimethyl-1,4,8,11-tetraazacyclotetradecane) (**2**). The X-ray crystal structures of the complex *trans*-$[Pt(\mathbf{2})Cl_2](ClO_4)_2$ and the analogue *trans*-$[Pt(\mathbf{1})Cl_2]Cl_2(ClO_4)_2\cdot 4H_2O$, resulting from chloroamine hydrolysis, are reported herein. The former is, we believe, the first X-ray crystal structure of a dichloroamine compound.

Experimental Section

Syntheses. The *trans*-(6-ammonio-6,13-dimethyl-1,4,8,11-tetraazacyclotetradecan-13-amine)platinum(II) perchlorate complex, *trans*-$[Pt(\mathbf{1}\text{-}H)](ClO_4)_3$, was prepared as described previously.[5]

***trans*-Dichloro(6,13-bis(dichloroamino)-6,13-dimethyl-1,4,8,11-tetraazacyclotetradecane)platinum(IV) Perchlorate, *trans*-$[Pt(\mathbf{2})Cl_2](ClO_4)_2$.** *Caution*! Complexes isolated in this synthesis are slightly shock sensitive and represent an explosive hazard. In a well-ventilated fume hood, a stream of chlorine gas was bubbled through a solution of *trans*-$[Pt(\mathbf{1}\text{-}H)](ClO_4)_3$ in water (500 mL). The solution became immediately cloudy, and the chlorine supply was maintained for 15 min. Following this, the solution was purged with nitrogen for 15 min to remove excess chlorine. An unstable, off-white precipitate was removed by filtration and carefully discarded. The filtrate was concentrated on a rotary evaporator to ca. 100 mL and acidified with perchloric acid (3 mL, 5 M). Precipitation of the product as colorless plates occurred within 1 day, and these were collected, washed with ethanol and diethyl ether, and dried in a vacuum desiccator. The yield was quantitative. Crystals of satisfactory quality for X-ray work were grown by slow evaporation of a solution of the complex in acetonitrile/water (9:1). Anal. Calcd for $C_{12}H_{26}Cl_8N_6O_8Pt$: C, 16.7; H, 3.0; N, 9.7. Found: C, 17.1; H, 3.2; N, 9.8. Electronic spectrum [water; λ_{max}, nm (ϵ, M^{-1} cm^{-1})]: 294 (780),

---

(1) (a) University of Newcastle. (b) University of Sydney.

(2) Drago, R. S. *J. Chem. Educ.* **1957**, *34*, 541.

(3) Schmitz, E. *Angew. Chem.* **1961**, *73*, 23.

(4) Kovacic, P.; Lowery, M. K.; Field, K. W. *Chem. Rev.* **1970**, *70*, 639.

(5) Bernhardt, P. V.; Lawrance, G. A.; Curtis, N. F.; Siriwardena, A.; Patalinghug, W. C.; Skelton, B. W.; White, A. H. *J. Chem. Soc., Dalton Trans.* **1990**, 2853.

0020-1669/92/1331-0631$03.00/0